JOURNAL OF PROPULSION AND POWER
Vol. 9, No. 2, March–April 1993

Experiments on Heat Transfer in a Cryogenic Engine Thrust Chamber

N. Sugathan,* K. Srinivasan,† and S. Srinivasa Murthy‡
Indian Institute of Technology, Madras 600036, India

Tests are conducted on a cryogenic engine using liquid oxygen as oxidizer and gaseous hydrogen as fuel with water as a coolant. The coolant flow passage of the thrust chamber is of milled channel configuration. Measured heat transfer results compare well with those predicted by a thermal analysis using the standard Bartz correlation and the Hess and Kunz correlation for hot gas side and coolant side heat transfer coefficients, respectively. This confirms the conclusions of a recent theoretical study by the authors in which a comparison of various heat transfer correlations was made.

Nomenclature

C = characteristic velocity, m/s
c_p = specific heat, kJ/kg K
D = diameter of cross section, m
D^* = throat diameter, m
h = convective heat transfer coefficient, W/m^2 K
k = thermal conductivity, W/m K
M = Mach number of flow
m = mass flow rate, kg/s
P = pressure, bar
Pr = Prandtl number
q = heat flux, kW/m^2
Re = Reynolds number
r_c = radius of curvature of throat section, m
T = temperature, K
t = wall thickness measured from exposed side, m
x = axial distance from throat, m
μ = absolute viscosity, kg m/s
τ = specific heat ratio

Subscripts
a = adiabatic
b = bulk
c = coolant
ch = chamber
g = hot combustion gas
inj = injection
t = total
w = wall
0 = stagnation value
1–4 = axial locations as in Fig. 1.

Superscripts
$'$ = temperature at depth of 1.5 mm on hot gas side
$''$ = temperature at depth of 0.5 mm on hot gas side

Introduction

IN the thermal design of cooling systems for the thrust chambers of rocket engines, reliable estimation of the coolant side and the hot gas side heat transfer coefficients is of great importance. In an earlier paper,[1] a critical evaluation of nine combinations of coolant side and hot gas side heat transfer correlations was carried out by the authors. By comparing it with limited published experimental data on engine cooling, it was found that the Hess and Kunz correlation[2,3] for the coolant side heat transfer coefficient and the standard Bartz correlation[4] for hot gas side heat transfer coefficient, are suitable for thermal design of regeneratively cooled cryogenic engines. However, it was felt that a detailed experimental verification was essential. In this article, such a study is presented with gaseous hydrogen as fuel, liquid oxygen as oxidizer, and water as the coolant. The present study also confirms the earlier contention that the above-mentioned pair of heat transfer coefficients is the best suitable for carrying out the thermal design.

Experimental Ground Test Setup

The configuration of a scaled model for static testing of the cryogenic engine is shown in Fig. 1, and the details are given in Table 1. The walls of the thrust chamber of this engine are made of a milled channel copper substrate enclosed in a stainless steel outer shell. The two materials are bonded together by vacuum brazing. Coolant entry and exit manifolds of the engine are tig-welded. A 16-element coaxial injector is used for admitting the fuel, gaseous hydrogen (GH2) and the oxidizer, liquid oxygen (LOX). A rigimesh porous face plate is used to provide transpiration cooling.

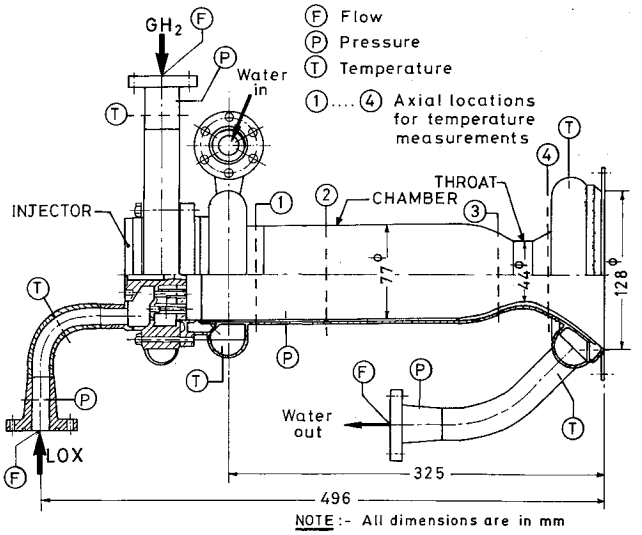

Fig. 1 Engine configuration.

Received May 31, 1991; revision received Sept. 25, 1991; accepted for publication Oct. 15, 1992.

*Refrigeration and Air Conditioning Laboratory, Department of Mechanical Engineering; currently Engineer SF, Liquid Propulsion Systems Center, Department of Space, Trivandrum 695547, India.

†Refrigeration and Air Conditioning Laboratory, Department of Mechanical Engineering; currently Associate Professor, Instrumentation and Services Unit, Indian Institute of Science, Bangalore 560012, India.

‡Professor and Head, Refrigeration and Air Conditioning Laboratory, Department of Mechanical Engineering.

Table 1 Configuration of the subscale engine

Sea level chamber area ratio	8.46
Characteristic length	84 cm
Nozzle contraction area ratio	3.09
Nozzle extension	*H*2 dump-cooled from area ratio 8.46–140
Injector	Coaxial multielement type with 18 elements
Igniter	Centrally mounted electrical type with preburner
No. of coolant channels	40

Coolant channel geometry	Cylindrical portion	Throat	Nozzle exit
Chamber wall thickness, mm	1.5	1.0	2.0
Channel width, mm	4.0	1.4	7.4
Channel height, mm	1.5	2.0	1.0

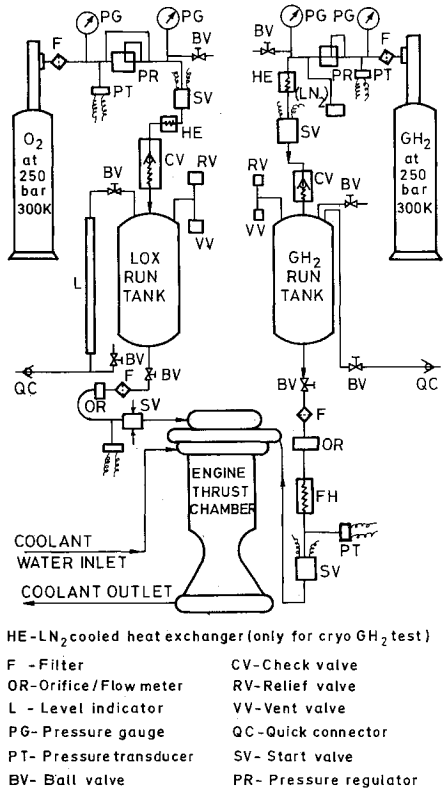

Fig. 2 Schematic of test setup.

A schematic diagram of the engine test setup is shown in Fig. 2. The experimental facility includes test stand structure, propellant feed system, auxiliary fluid circuits, and instrumentation. The test stand structure supports the engine in the horizontal position and the thrust is transmitted to it through suitable load cells. The propellant feed system consists of GH2 and LOX subsystems. Each subsystem is composed of facilities for pressurization, filling, draining, cool down, purging, and monitoring of various parameters. Other main components of the test facility are the high-pressure run tank for storing GH2 and the superinsulated LOX tank. LOX is transferred to the engine by an oxygen gas pressurization system. The liquid feed lines are insulated with polyurethane foam. Helium gas is used for the pilot pressure source for regulator and also command pressure to cryogenic valves.

Locations of temperature, pressure, and flow transducers on the engine hardware are also shown in Fig. 1. Pertinent details of instrumentation are given in Table 2. Platinum resistance sensors are used for fuel and oxidizer temperature measurement. Thermocouples are used for coolant and chamber wall temperature measurement. In four axial positions of the chamber identified in Fig. 1, three thermocouples each

Table 2 Details of instrumentation

Pressure transducers	
Type	Thin film/strain gauge
Accuracy class	±0.5%
Temperature transducers	
Thermocouple types	Copper-Constantan and Chromel-Alumel
Gauge	24 swg
Resistance temperature devices (RTD)	
Type	Platinum resistance
Sensitivity	0.00395 Ω/°C
Response time	100/300 ms
Accuracy	0.75% or 1%
Flowmeters	
Type	Turbine
Accuracy	0.15%
Digital panel meter (DPM)	
Type	Duel slope integrating type
Display	3.5 digit
Accuracy	±0.1%

Table 3 Test conditions

Parameter	Value
Chamber pressure	10 ± 0.2 bar
LOX injection pressure and temperature	10 ± 0.2 bar and 90 K
GH2 injection pressure and temperature	14.5 ± 0.2 bar and 300 K
Injection velocity ratio (fuel/oxidizer)	41
LOX flow rate	0.58 ± 0.01 kg/s
GH2 flow rate	0.097 ± 0.0002 kg/s
Coolant water flow rate	6 kg/s
Coolant temperature	310 K
Nominal firing time	50 s (test 1) 200 s (test 2)

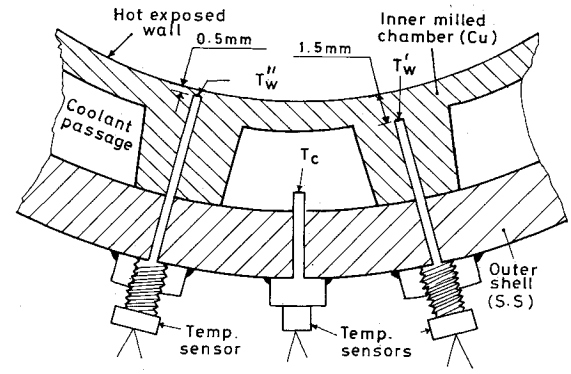

Fig. 3 Temperature probe locations.

are installed as shown in Fig. 3. High precision in locating the thermocouples is ensured by the use of a computerized numerically controlled milling machine to drill the holes. The thermocouples are spot-welded to the flat bottom of the holes.

Experimental Procedure

The engine is tested in a pressure-fed mode for a 50- and 200-s duration. The test conditions are given in Table 3. The propellant flow rates, and thereby the combustion chamber pressure, are maintained constant during both tests by setting the injector upstream pressures at predetermined values. Also, the water flow rate is maintained at 6 kg/s during tests. This is achieved by calibrating the entire coolant line with the engine hardware prior to the test.

Tests are conducted according to a predetermined test sequence. Countdown starts 30 min before the start of engine ignition, and ends 10 min after the engine firing. Steady conditions are observed about 10 s from the start. Data obtained

from the experiments are used in the thermal analysis for making a comparison with the predictions made based on the authors' earlier paper.[1]

Calculation Procedure

Heat transfer calculations using the measured temperature data are done considering one-dimensional, steady-state heat conduction in the radial direction as already described by the authors.[1]

Considering the wall thickness and rib-effect in heat transfer, the coolant side wall temperature $T_{w,c}$ and exposed wall temperature $T_{w,g}$ are extrapolated using measured temperatures inside the wall. Here, the temperature gradient in the ribs between coolant channels is taken as linear.

For instance, near the inlet point of coolant, the measured values of temperatures are

$$T''_{w,1} = 440 \text{ K}$$

$$T'_{w,1} = 410 \text{ K}$$

$$T_{c,1} = 310 \text{ K}$$

and the extrapolated temperatures are

$$T_{w,g} = 460 \text{ K}$$

$$T_{w,c} = 400 \text{ K}$$

Making use of one-dimensional, steady-state heat conduction equation in the copper shell in the direction of local radius of curvature, the local heat flux is calculated as

$$q = k_w(T_{w,g} - T_{w,c})/t = (0.35 \times 60)/0.0015 = 14 \times 10^3 \text{ kW/m}^2 \quad (1)$$

Also

$$q = h_{g,t}(T_{w,a} - T_{w,g}) \quad (2)$$

which yields

$$h_{g,t} = 4.76 \text{ kW/m}^2 \text{ K}$$

where $T_{w,a}$, the adiabatic wall temperature of gas stream at the location, is calculated using

$$T_{w,a} = T_g + (T_{ch} - T_g)\Phi_R \quad (3)$$

where Φ_R is the boundary-layer recovery factor which varies from 0.9 to 0.99 depending on the Prandtl number of the flowing gas. Equation (3) is a modification of standard equation[4]

$$T_{w,a} = T_{ch}\Phi_R \quad (4)$$

This modification is done to account for the influence of static gas temperature T_g, which is calculated from Ref. 4

$$T_g = T_{ch}/[1 + M^2(\tau - 1)/2] \quad (5)$$

In the present work T_{ch}, the adiabatic combustion temperature, which is a function of mixture ratio ($O/F = 0.6$) and chamber pressure, is taken from Ref. 8. $T_{w,a}$ calculated the same way is equal to 3398 K.

Also, by considering heat balance in one-dimensional steady state

$$q = h_c(T_{w,c} - T_c) \quad (6)$$

whereby

$$h_c = q/(T_{w,c} - T_c) = 155 \text{ kW/m}^2 \text{ K} \quad (7)$$

Results and Discussion

Figures 4–7 present the pressure and temperature data obtained during the 50-s engine test, and Figs. 8–11 show similar data obtained from the 200-s engine test. The combustion chamber pressure during both the tests was maintained at 10 bar. This was achieved because pressure drops of both propellants in injectors could be predicted accurately, and the coefficient of discharge for both propellants were known precisely. The temperatures recorded from the inner copper shell at different radial depths from the surface exposed to hot gas show similar trend. Temperatures are transient up to 10 s from the start of engine firing before steady state is attained. Other properties of the combustion product remain constant; the heat transfer coefficient in the hot gas side is a function of chamber pressure only.

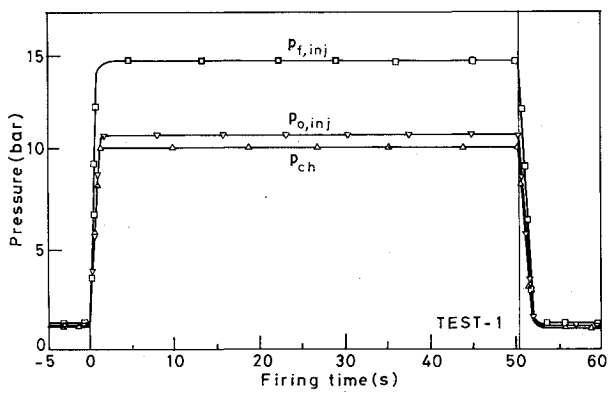

Fig. 4 Pressure variation as a function of time in test 1.

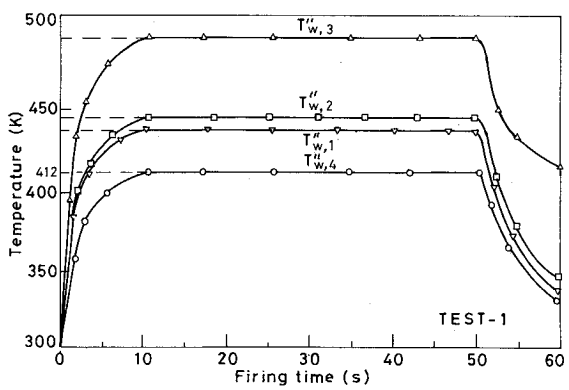

Fig. 5 Wall temperature variation as a function of time in test 1 at 0.5-mm depth.

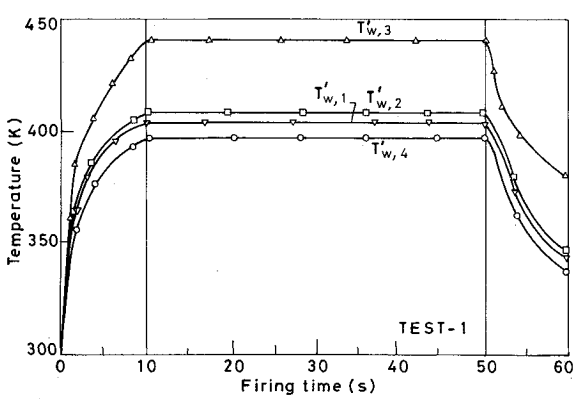

Fig. 6 Wall temperature variation as a function of time in test 1 at 1.5-mm depth.

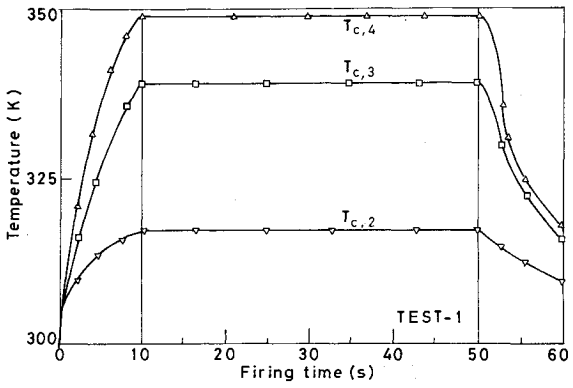

Fig. 7 Coolant temperature variation as a function of time in test 1.

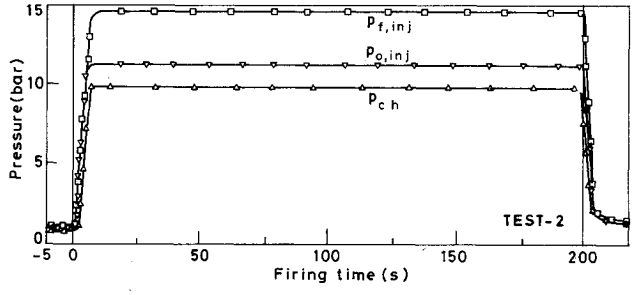

Fig. 8 Pressure variation as a function of time in test 2.

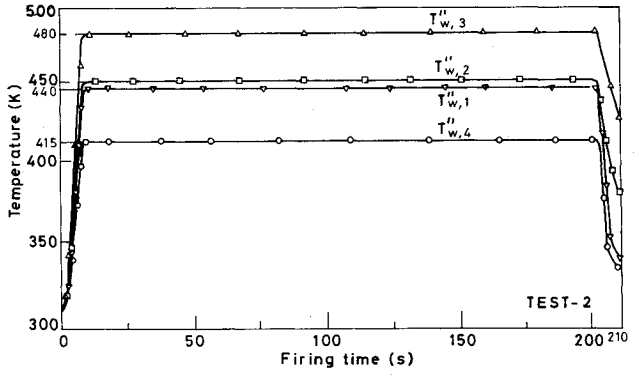

Fig. 9 Wall temperature variation as a function of time in test 2 at 0.5-mm depth.

The experimentally determined hot gas side heat transfer coefficients are compared with the standard Bartz correlation[4]

$$h_g = (0.026/D^{0.2})(\mu^{0.2}c_{p,g}/Pr^{0.6})(P/C)^{0.8}(D^*/r_c)^{0.1}(D^*/D)^{1.8}\phi \quad (8)$$

where ϕ is the correction factor for property variation across the boundary layer, given by

$$\phi = [1 + M^2(\tau - 1)/2]^{-0.12}/\{0.5 + 0.5(T_{w,g}/T_0) \cdot [1 - M^2(\tau - 1)/2]\}^{0.68} \quad (9)$$

P is the chamber static pressure measured at an axial location of 50 mm from the coolant inlet as shown in Fig. 1. C is calculated at stagnation conditions as given in Ref. 4.

The coolant side heat transfer coefficients derived from the experiments are compared with the Hess and Kunz correlation[2,3]

$$h_c = (k_c/D)[0.0208Re_c^{0.8}Pr_c^{0.4}(1 + 0.01457\mu_w/\mu_b)] \quad (10)$$

As seen in Fig. 12, h_c derived from tests, closely matches with the predictions from Eq. (10). The Sieder-Tate correlation[4]

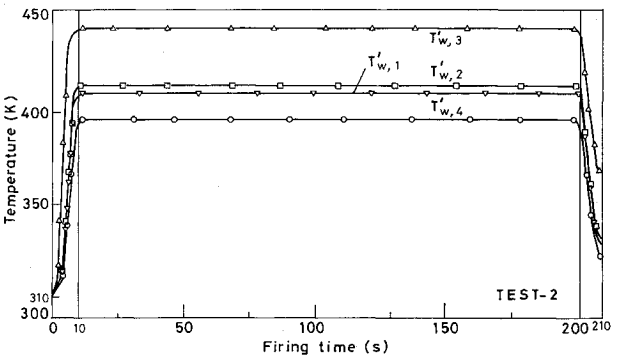

Fig. 10 Wall temperature variation as a function of time in test 2 at 1.5-mm depth.

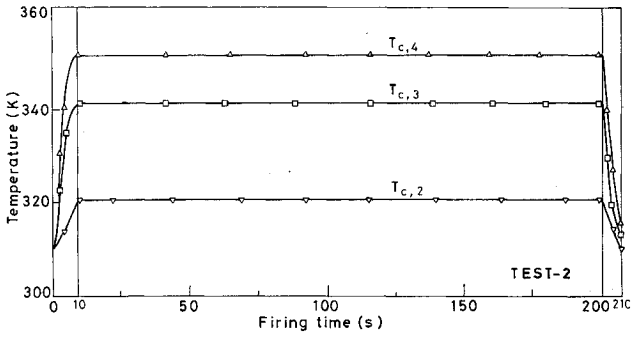

Fig. 11 Coolant temperature variation as a function of time in test 2.

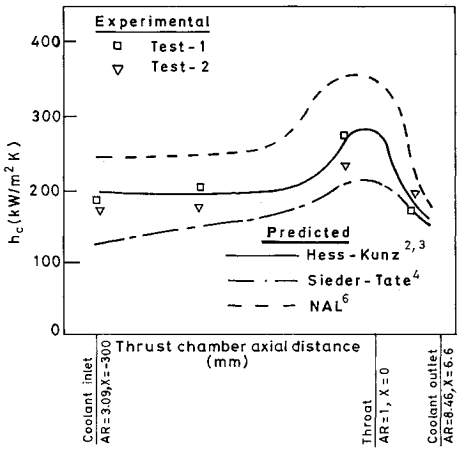

Fig. 12 Comparison of coolant side heat transfer coefficients.

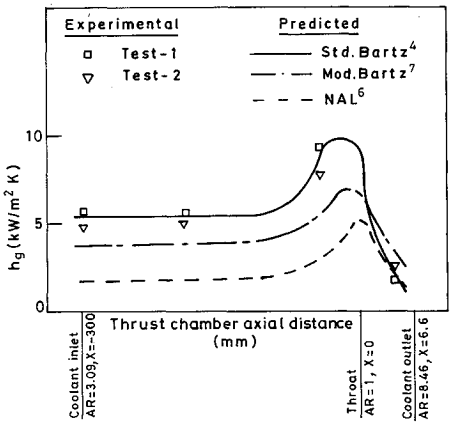

Fig. 13 Comparison of hot gas side heat transfer coefficients.

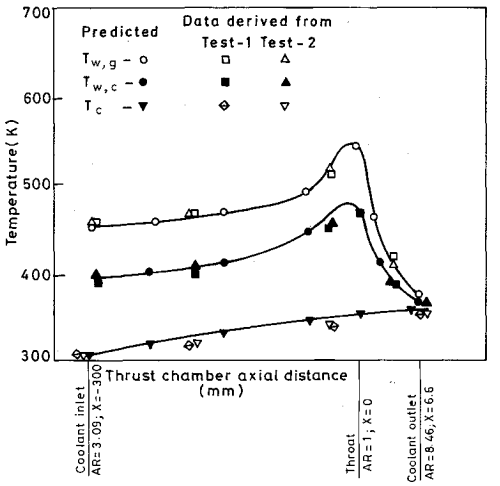

Fig. 14 Comparison of temperatures at various locations.

overpredicts the heat transfer coefficient, whereas, the National Aerospace Laboratory (NAL), Japan correlation[6] underpredicts the heat transfer coefficient. Similarly, the values of h_g derived from test data match well with the predictions of Eq. (8) as shown in Fig. 13. Both modified Bartz[7] and NAL[6] correlations underpredict the gas side heat transfer coefficient. Coolant and wall temperature variations predicted from the one-dimensional thermal analysis[1] using the pair of standard Bartz, and Hess, and Kunz correlations are compared with measured values in Fig. 14. In the case of temperatures, the deviations are within $+10.7\%$ to -1.8%.

Conclusions

Test results obtained on a cryogenic engine with water as coolant match well with the predictions made from a one-dimensional thermal analysis using the standard Bartz equation for the hot gas side heat transfer coefficient, and the Hess and Kunz correlation for the coolant side heat transfer coefficient. It is suggested that this pair of correlations may be used for the thermal design of thrust chambers.

References

[1]Sugathan, N., Srinivasan, K., and Srinivasa Murthy, S., "Comparison of Heat Transfer Correlations for Cryogenic Engine Thrust Chamber Design," *Journal of Propulsion and Power*, Vol. 7, No. 6, 1991, pp. 962–967.

[2]ARQUARDF Corp., "Thrust Chamber Cooling Techniques for Space Craft Engines: Final Report," NASA CR-50959, July 1963.

[3]Hess, H. L., and Kunz, H. R., "A Study of Forced Convection Heat Transfer to Super-Critical Hydrogen," *Transactions of the American Society of Mechanical Engineers, Journal of Heat Transfer*, Vol. 87, Feb. 1965, pp. 41–48.

[4]Huzel, D. K., and Huang, D. H., "Design of Liquid Propellant Rocket Engines," NASA SP-125, 1971.

[5]Yanagawa, K., Fujito, T., Katsuda, H., and Miyjima, H., "Development of LOX/LH2 Engine LE-5," AIAA/SAE/ASME 20th Joint Propulsion Conf., AIAA Paper 84-1223, Cincinnati, OH, June 11–13, 1984.

[6]Kumakawa, A., Niino, M., Yatsuyanagi, N., Gomi, H., Sakamoto, H., and Sasaki, M., "A Study of the Cooling of Low Thrust LO2/LH2 Rocket Engine," *Proceedings of the 13th International Symposium on Space Technology and Science*, Tokyo, 1983, pp. 301–306.

[7]Steer, T. E., "The Design and Manufacture of a Liquid Hydrogen Thrust Chamber," *Space Flight*, Vol. 1, Feb. 1970, pp. 135–142.

[8]Gordon, S., and McBride, B. J., "Theoretical Performance of Liquid Hydrogen with Liquid Oxygen as Rocket Propellant," NASA TM-5-21-59E, March 1959.